Thermal Analysis and Testing of Different Designs of Lanthanum Hexaboride Hollow Cathodes

Ugur Kokal*, Nazlı Turan, Murat Celik
Department of Mechanical Engineering
Bogazici University
Istanbul, Turkey
*Corresponding Author: ugur.kokal@boun.edu.tr

Hüseyin Kurt
Department of Engineering Physics
Istanbul Medeniyet University
Istanbul, Turkey

***Abstract*—Electric propulsion systems provide a higher delta-V for the same mass of propellant when compared to chemical propulsion systems due to their higher I_{sp} levels. Many electric propulsion systems utilize cathodes as electron source. Hollow cathodes generate electron current through thermionic emission mechanism. In this study conventional hollow cathode designs are investigated numerically and experimentally. Considering the problems that are encountered with the conventional designs, a new hollow cathode design is developed, which is called *coaxial hollow cathode*. Operational parameters of the coaxial cathode are investigated experimentally.**

Keywords— electric propulsion, hollow cathode, thermionic emission, thermal analysis.

I. Introduction

Space propulsion systems are used for maneuvers of the spacecraft in orbit or during deep space missions. Most commonly used space propulsion systems are chemical propulsion systems and electric propulsion systems. While the chemical propulsion systems are suitable for launch vehicles and maneuvers that require fast burns, electric propulsion systems can provide higher delta-V with less propellant resulting in cost savings [1].

Electric propulsion systems produce thrust by generating plasma and accelerating the ions from the plasma with the use of electric and magnetic fields [2]. Electric propulsion devices are operated with an electron source called cathode which is responsible for providing electrons for ionization and neutralization. In Kaufman type ion thrusters, propellant gas is ionized with an internal cathode, also an external cathode provide neutralization [3]. External cathodes are utilized for the ionization and neutralization at Hall effect thrusters [4].

Hollow cathodes are preferred for the operation as an electron source. In hollow cathodes electrons are generated through thermionic emission process. Materials with low work function are utilized as the emitter elements. At high temperatures, these materials emit electrons. The emission current density is determined by the temperature and the work function of the emitter material. Commonly used emitter materials are barium-oxide impregnated tungsten (BaO-W) and lanthanum hexaboride (LaB_6). BaO-W has very low work function of 2.06 eV [5-6]. However, the high sensitivity of BaO-W to the impurities in the propellant shortens the hollow cathode life time [6-7]. LaB_6 emitters are resistant to impurities and provide longer lifetime, therefore they become prevalent choice as emitter material [8-13]. However as the work function of LaB_6 is around 2.67 eV, higher temperatures are needed for operation [14]. Emission current density can be calculated from the Richardson-Dushman equation:

$$j = A{T_w}^2 e^{-\frac{e\varphi}{kT_w}} \tag{1}$$

where, j is the emission current density, T_w is the emitter wall temperature, φ is work function in eV, and k is Boltzmann constant [15]. According to Richardson-Dushman equation, emission current densities for different emitter materials at different temperatures are shown in Fig 1.

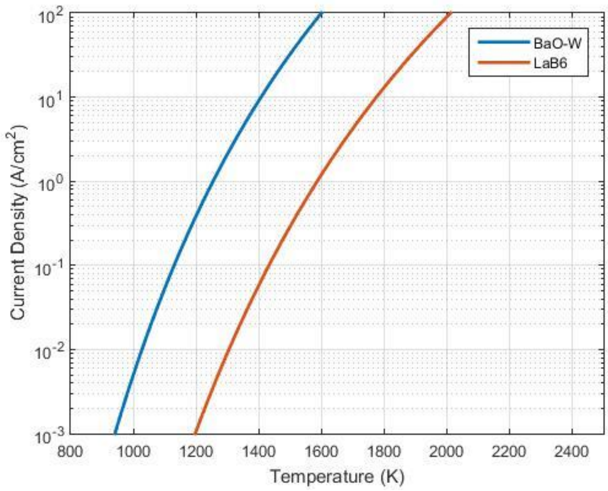

Fig. 1. Emission current density of BaO-W and LaB_6 vs. temperature

Developed hollow cathodes are being used with the thrusters developed at the Bogazici University Space Technologies Laboratory (BUSTLab), therefore expected cathode discharge current is about 1-3 A. Considering the available emitter materials, the required emission current density should be around 5-6 A/cm^2. As seen in the Fig. 1, required temperature is higher than 1100 °C with BaO-W emitter, however LaB_6 emitters require temperatures higher than 1500 °C.

The emitter material is designed as a cylindrical insert part to be placed within a conductive cathode tube (Fig. 2). Above the required temperatures, electrons extracted from the emitter material collide with the neutral particles of the propellant and by the ionization of the neutrals a quasi-neutral plasma is generated within the cathode tube. As the electrons are extracted from the emitter surface, a sheath formation occurs at the emitter surface. Therefore, a non-zero electric field develops at the wall, which enhances electron emission. As the electrons are accelerated from the emitter wall to the plasma by the electric field, ions are accelerated towards the emitter surface. Collision of the ions to the emitter surface provides a heating source for the emitter, thus a self-heating mechanism for the cathode operation is established. The self-heating mechanism arranges itself according to the extracted electron current. Increased discharge current from the cathode increases the plasma potential within the insert region, thus increases the number of extracted electrons from the emitter surface [16].

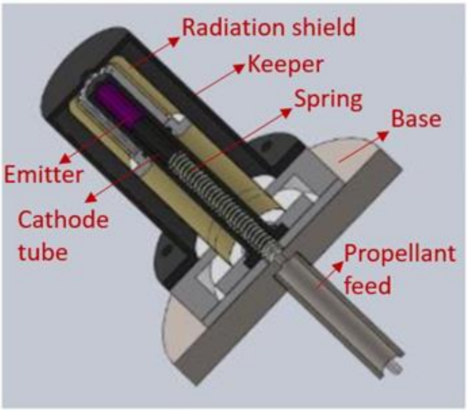

Fig. 2. Section view of hollow cathode

The quasi-neutral plasma within the insert region is sustained by a keeper tube, which encloses the cathode tube. A positive voltage, which is higher than the plasma voltage within the insert region, is applied to the keeper, so that an electron flow from the plasma is generated. Because of the electron flow from the plasma to the keeper, the plasma voltage within the insert region is kept at desired level, which sustains the self-heating mechanism.

II. CONVENTIONAL HOLLOW CATHODE DESIGN

As the temperature of the insert has to be high enough for the thermionic emission, a heater assembly is used. Joule heating is the most common method for the heating process. In this method a heater coil is wrapped around an insulator ceramic, which covers the region around the emitter material. As the heater element, refractory metals such as tungsten, tantalum and rhenium are used [17].

Several different conventional heater designs are built at BUSTLab, and effectiveness of these designs are compared both numerically and experimentally. According to these results, several improvements to the design are made. As the emitter material a LaB_6 tube with 2 mm inner diameter, 4 mm outer diameter and 10 mm length is utilized. Emitter material is placed inside a graphite cathode tube with 4mm inner diameter, 6 mm outer diameter and 48 mm length.

Fig. 3. a) First conventional heater design, b) Second conventional heater design

In Fig. 3, two different conventional hollow cathode heaters that are built at BUSTLab are shown [18]. In the first design (Fig. 3a), the heater element is constructed with alumina tubes with two holes and a tantalum wire with 0.25 mm diameter. Alumina tubes are aligned around the cathode tube, and tantalum wire is sewed into the holes of these tubes. A tantalum shield is placed around the heater structure for radiative shielding. Heater element and radiative shield is supported with a macor ceramic holder part. Electrical connection is supplied by the both ends of the tantalum wire that is insulated by alumina tubes and spine beads. In the second conventional heater design (Fig. 3b), a tantalum wire is wrapped around the helical grooves of an insulator ceramic part, which is made of shapal. Upper end of the tantalum wire makes contact with the cathode tube, thus the cathode tube provides the electrical connection. Bottom end of the tantalum wire, which is insulated with alumina tubes and spine beads, completes the electrical circuit. The heater wire is insulated with alumina or shapal outer sleeves. In both cathode designs, the heater region is covered with tantalum radiative shields. The cathode tube is fastened with a macor holder to the base plate. As keeper, a graphite tube is utilized, which is mounted on a second macor holder.

III. CONVENTIONAL HOLLOW CATHODE TESTS

Effectiveness of different heater designs is investigated experimentally. Tests are conducted inside the BUSTLab vacuum chamber, which is 1.5 m in diameter and 2.7 m in length [19]. During the tests the pressure inside the chamber is kept around 5×10^{-5} torr. Argon is used as propellant gas. Different heater designs are tested several times by heating the cathode and initiating electron extraction from the cathode. After the tests, keeper assembly is disassembled and the heater region is investigated.

In the first conventional heater design (Fig. 4), it was seen that the sharp turns at the bending points of the heater wire are damaged at high temperatures, which shortens the cathode lifetime. Thermal contact at bending regions decreases as the temperature of the heater wire increases. Decreased thermal contact causes temperature rise and non-uniform temperature profile, which damages the heater structure. Also, even if the return ends of the heater wire are well insulated, joining points between the return wire and heater assembly creates a weak point, which is damaged at high temperatures.

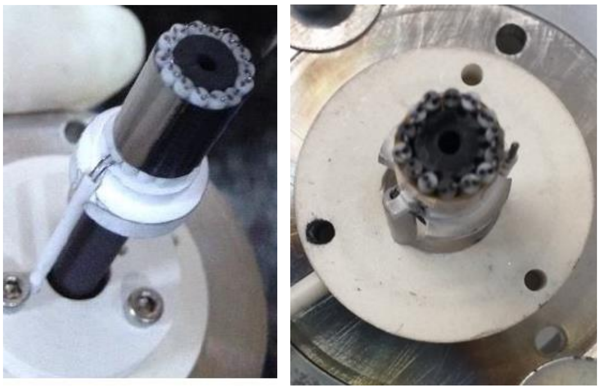

Fig. 4. a) First conventional heater design, b) Damaged heater after the tests

In the second conventional heater design (Fig. 5), sharp turns are avoided, therefore longer cathode lifetimes are achieved. However, the joining points at the both ends of the heater wire are damaged after numerous heating processes.

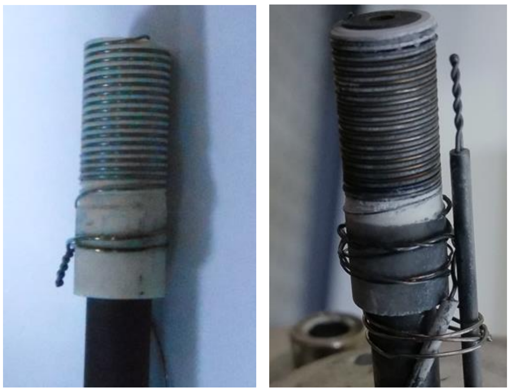

Fig. 5. a) Second conventional heater design, b) Damaged heater after the tests

IV. Coaxial Hollow Cathode Design

Due to the problems that are encountered with the conventional heater designs, a coaxial hollow cathode design is developed (Fig. 6). In this design any sharp turns of the heater wire are avoided, therefore any critical weak points are eliminated. In the coaxial cathode design, a coaxial graphite part is used to provide electrical connection to the heater wire. Cathode tube and coaxial graphite part are separated with an alumina insulator sleeve. Heater wire is wrapped around the grooves of the graphite part and shapal insulator. Grooves of the shapal and graphite parts are aligned for smooth transition. Heater wire is insulated with a shapal cover part. As the wire is completely covered with insulator parts, any thermal contact loss that is caused by the thermal expansion is avoided. Thus, more uniform temperature profile within the heater region is obtained, which also extends cathode lifetime. Electrical connection is achieved by using steel screws; therefore a more rigid electrical connection is obtained.

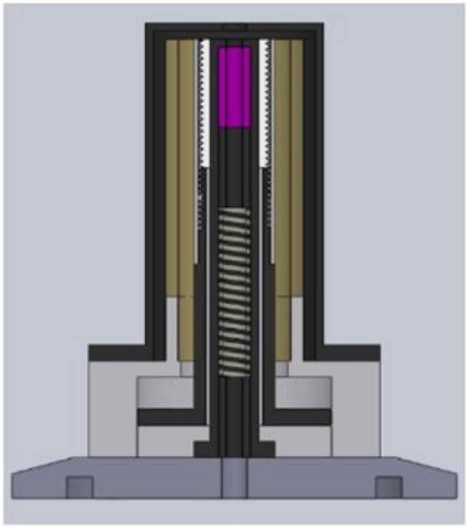

Fig. 6. Cross-sectional view of the coaxial hollow cathode

V. Modelling and Analysis of Cathode

Numerical analyses of different hollow cathode designs are conducted using COMSOL Multiphysics. In the analyses, 2D axisymmetric computational domains are used as shown in Fig. 7.

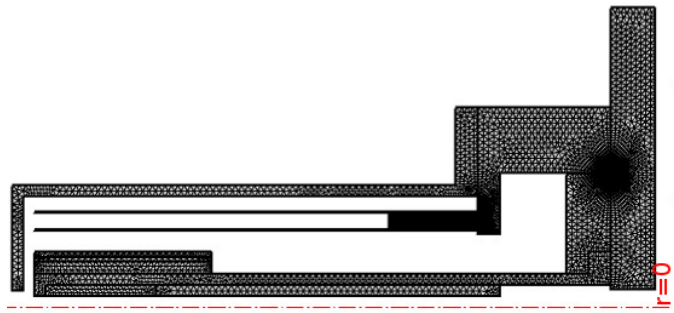

Fig. 7. 2D axisymmetric mesh domain

Temperature and heat flux distributions are investigated by conducting thermal analyses. Necessary heater power inputs are applied at each case, so that inner surface of the insert is kept at 1500 °C, which is required for the initiation of the thermionic emission. Thermal conductivity of the cathode components vary with temperature as seen in Fig. 8. Surface emissivity and thermal conductivity values of the cathode components are shown in Table 1.

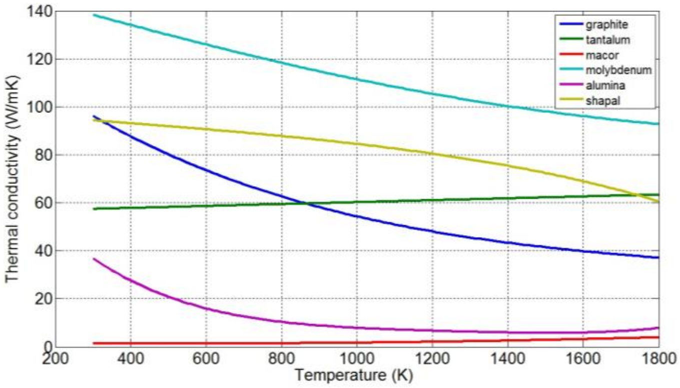

Fig. 8. Thermal conductivity of cathode parts vs. temperature

Heat flux distributions for different hollow cathode designs are shown in Fig. 10. It can be seen that the additional graphite part in the coaxial design increases the cross section of the thermal path from the heater region to the cathode base, therefore conductive heat transfer to the cathode base is increased, which also increases the required power input (Fig. 10c). However, mounting the graphite return part and keeper on a macor insulator decreases the heat loss to the base plate.

TABLE 1. Surface emissivity and thermal conductivity values

Materials	**Emissivity**	**Thermal Conductivity at 300 K [W/(m K)]**	**Thermal Conductivity at 1700 K [W/(m K)]**
Graphite	0.7	96.25	38.38
Alumina	0.9	36.96	6.53
Tantalum	0.2	57.4	62.97
Molybdenum	0.1	138.32	94.3
Shapal	0.83	94.39	65.08
Macor	0.87	1.44	3.54

According to the thermal analysis, the main heat loss mechanism from the hollow cathode is the radiative heat transfer from the keeper surface; therefore radiative shields are essential for hollow cathode operation. In Fig 11, radiosity values of the cathode surfaces for different shield designs are shown. In Fig. 11a, two concentric tantalum shields are used. In this design required power input is about 180 W. In Fig. 11b, molybdenum radiative shields are used. As the surface emissivity of the molybdenum is lower than tantalum, a better radiative shielding is achieved and the required input power decreases to 170 W. In both designs a significant percentage of the radiative heat transfer occurs between the upper surface of the ceramic cover of the heater and the inner surface of the keeper. In Fig. 11c, the ceramic cover part is partially covered with a molybdenum shroud, which decreases the required power input to 150 W.

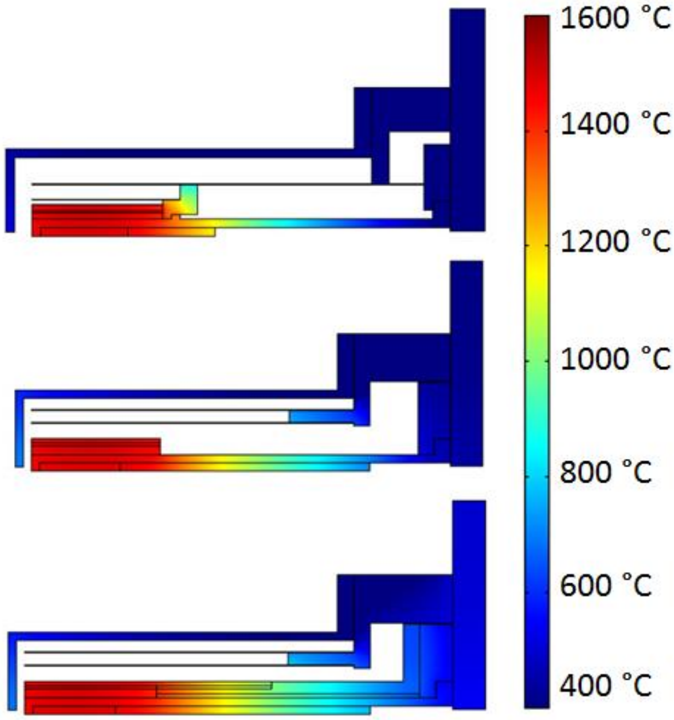

Fig. 9. Temperature distribution, Top: First conventional heater design, Middle: Second conventional heater design, Bottom: Coaxial hollow cathode design

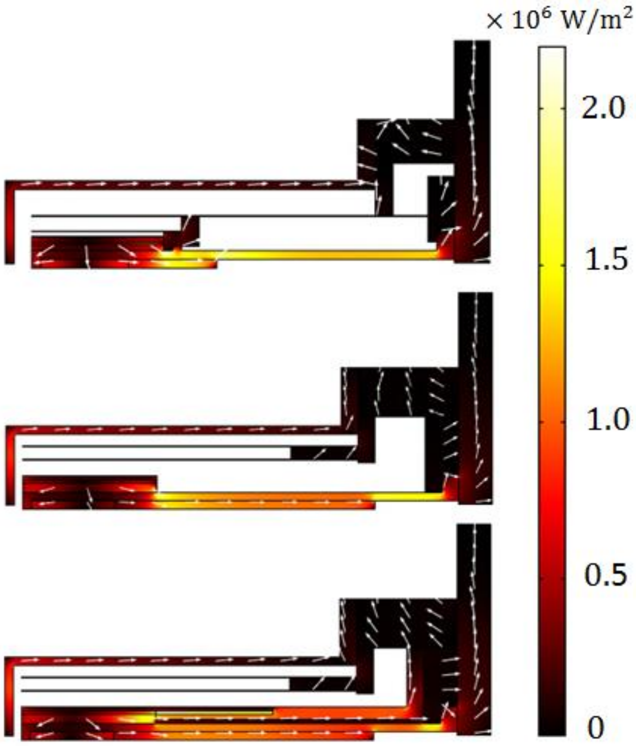

Fig. 10. Heat Flux, Top: First conventional heater design, Middle: Second conventional heater design, Bottom: Coaxial hollow cathode design

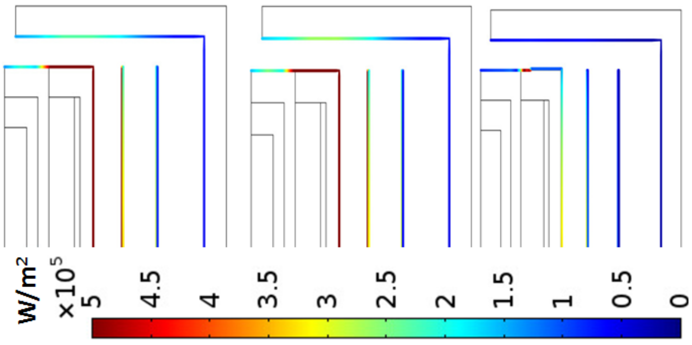

Fig. 11. Radiosity of cathode inner surfaces, a) Two concentric tantalum shields, b) Two concentric molybdenum shields, c) Two concentric molybdenum shields with molybdenum inner cap

In order to initiate the self-heating mechanism, quasi-neutral plasma has to be generated within the insert region. This plasma is sustained by the electron flow from the emitter surface and the electron extraction from the plasma through the orifice channel. For the electron extraction from the insert plasma, an outer electrical potential has to be applied. Therefore, a voltage that is higher than the plasma voltage is applied to the keeper. The orifice region has to be designed in a way, so that the keeper voltage can reach the insert plasma. In Fig. 12, the electrical potential around the orifice region before the plasma initiation is shown.

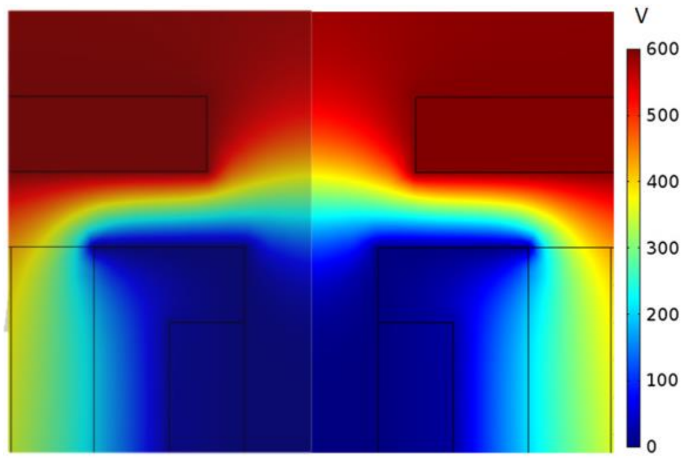

Fig. 12. Electrical potential distribution in the orifice region of the cathode

VI. Experimental Analysis

Operational parameters of the coaxial hollow cathode are investigated experimentally by using a virtual anode. The virtual anode is a hollow cylinder that is made of perforated steel plate, and mimics the plume plasma of the thruster. The virtual anode is aligned with the exit plane of the keeper as shown in Fig. 13. Further tests are conducted with thrusters that are developed at BUSTLab [20-21].

Tests are performed with Argon propellant. A floating electrical setup is used in the tests (Fig. 14). Three separate power sources are utilized for the heater, keeper and discharge circuits. Also, the floating common ground voltage is measured with a multimeter. The tests begin with the heating process, which takes several minutes. During the heating process Argon gas is fed to the cathode, and a keeper voltage is applied. Electron extraction from the cathode initiates after the cathode reaches to the necessary temperature. After the heating process is completed, the heater power is turned off.

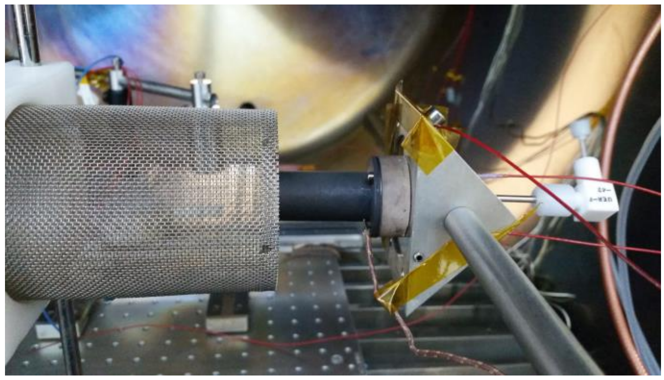

Fig. 13. Hollow cathode assembly during virtual anode tests

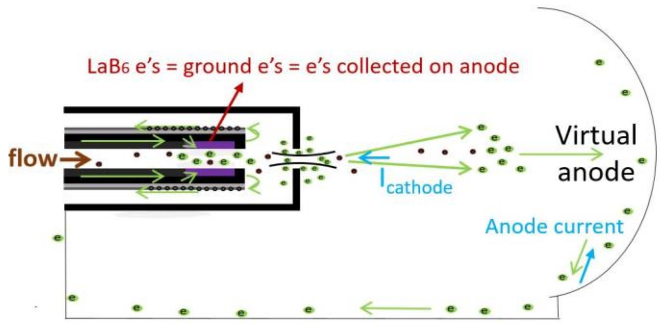

Fig. 14. Hollow cathode and virtual anode schematic

For the tests, the ground current is measured as the biased anode current 1.2 A plus the keeper current 1.4 A while the anode voltage arranges itself to appropriate values as the mass flow rate changes. The magnitude of the cathode electron current is determined by the biased anode current because the anode and the cathode are connected by the negative leads of the power supplies.

The mass flow rate is varied and the anode voltage is observed as in Fig. 15. As the flow rate is increased, the anode current changes more dramatically. The cathode voltage has a negative value and changes as the electrons are extracted from the LaB_6 insert. When the flow is low, the cathode cannot sustain 1.2 A, and arranges itself to lower values as shown in the Fig. 16. After a certain flow rate, there are enough electrons to satisfy the preset current, 1.2 A. The current jump is observed while the resistance inside the cathode decreases with the increased flow rate. The keeper voltage also decreases and the sheath disappears as all the electrons emitted are attracted by the anode. The negative cathode voltage becomes more negative with the current jump. As a result, the voltage difference increases due to the sharp increase in the cathode voltage magnitude.

Depending on the results, it can be said that the electron current extracted from the cathode is equal to the current collected on the anode cup. Higher electron current is desired for the thruster operation and the cathode mass flow rate is determined to be 2.2 sccm for Argon propellant. The changes in power consumption are shown in Fig. 17.

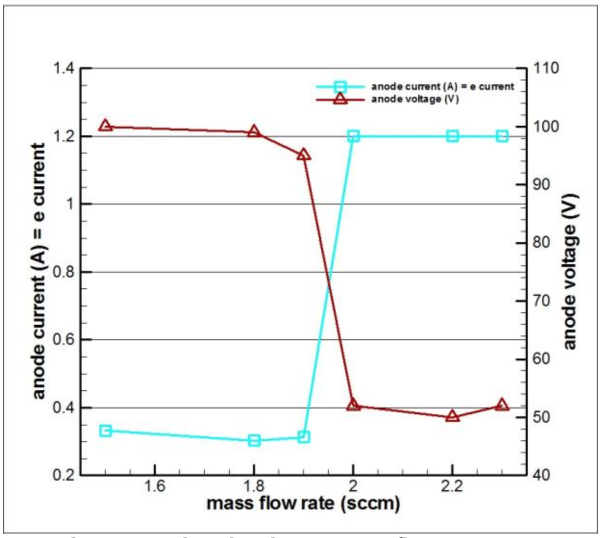

Fig. 15. Anode current and anode voltage vs. mass flow rate

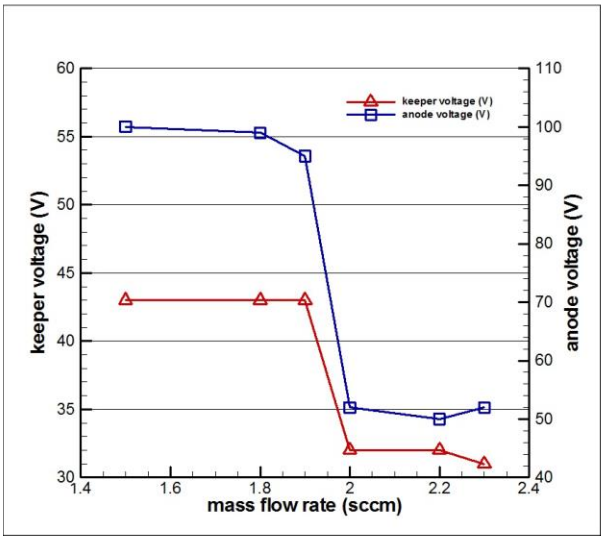

Fig. 16. Anode current and anode voltage vs. mass flow rate

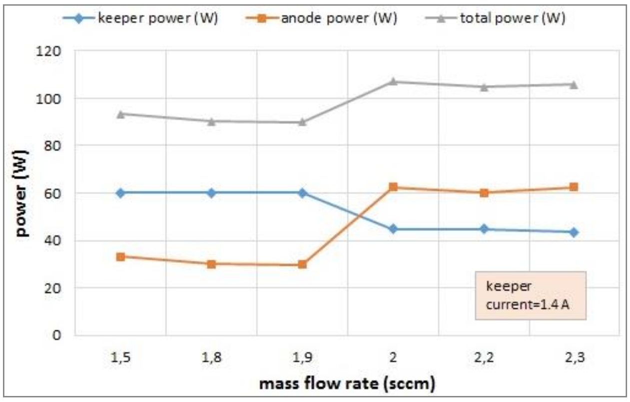

Fig. 17. Power consumption vs. mass flow rate

VII. Conclusion

Several hollow cathode designs are investigated both numerically and experimentally. Effectiveness of different heater designs is compared. Also, critical failure points are investigated. Based on the problems encountered during tests with the conventional hollow cathode designs, a novel hollow cathode is developed. Comprehensive numerical analyses of this design are performed. Also, several possible improvements concerning the required power input and heat loss are investigated. The developed coaxial hollow cathode requires higher initiation power; however it provides a more durable design with an increased lifetime. According to the experimental measurement results, the developed cathode can supply the desired electron current levels for different mass flow rates.

Acknowledgement

The authors would like to thank Turkish Scientific and Technological Research Council (TUBITAK) for their partial support to this work under project number 112M862.

References

[1] Martinez-Sanchez, M. and Pollard, J.E., “Spacecraft Electric Propulsion-An Overview,” Journal of Propulsion and Power, Vol. 14, No. 5, 1998, pp. 688–699.

[2] Jahn, R. G. and Choueiri, E. Y., “Electric Propulsion", Encyclopedia of Physical Science and Technology, No. 3589, 2002.

[3] Choueiri, E. Y., “A Critical History of Electric Propulsion: The First 50 Years (1906-1956)”, Journal of Propulsion and Power, Vol. 20, No. 2, 2004, pp. 193-203.

[4] Sommerville, J. D., “Hall-Effect Thruster-Cathode Coupling: The Effect of Cathode Position and Magnetic Field Topology”, Ph.D. Thesis, Michigan Technological University, Houghton, MI, USA, 2009.

[5] D. M. Goebel and I. Katz, “Fundamentals of Electric Propulsion: Ion and Hall Thrusters”, JPL Space Science and Technology Series, New York, USA, 2008.

[6] D. M. Goebel and R. M. Watkins, “Compact Lanthanum Hexaboride Hollow Cathode,” Review of Scientific Instruments 81, 2010.

[7] M. T. Domonkos, “Evaluation of Low-Current Orificed Hollow Cathodes,” Ph.D. Thesis, The University of Michigan, Ann Arbor, MI, 1999.

[8] J. E. Polk, D. M. Goebel, R. Watkins, K. Jameson, L. Yoneshige, J. Przybylowski, and L. Cho, “Characterization of Hollow Cathode Performance and Thermal Behavior,” in 42nd Joint Propulsion Conference and Exhibit, Sacramento, CA, 2006, also AIAA–2006–5150

[9] D. M. Goebel, R. M. Watkins, and K. K. Jameson, "LaB_6 Hollow Cathodes for Ion and Hall Thrusters," Journal of Propulsion and Power 23, 552–558, 2007.

[10] D. J. Warner, "Advanced Technologies for Next Generation Electric Propulsion Technology," M.S. Thesis, Air Force Institute of Technology, Dayton, OH, 2008.

[11] D. J. Warner, R. D. Branam, and W. A. Hargus, "Ignition and Plume Characteristics of Low-Current Cerium and Lanthanum Hexaboride Hollow Cathodes," Journal of Propulsion and Power 26, 130–134, 2010.

[12] D. M. Goebel and E. Chu, "High Current Lanthanum Hexaboride Hollow Cathodes for High Power Hall Thrusters," in 32nd International Electric Propulsion Conference (Wiesbaden, Germany, 2011) IEPC-2011-053.

[13] D. G. Courtney, "Development and Characterization of a Diverging Cusped Field Thruster and a Lanthanum Hexaboride Hollow Cathode," M.S. Thesis, Massachusetts Institute Of Technology, Cambridge, MA, USA, May, 2008.

[14] D. Jacobson and E. Storms, "Work Function Measurement Of Lanthanum-Boron Compounds," IEEE Transactions on Plasma Science 6, 191–199, 1978.

[15] Neamen, D. A., "Semiconductor Physics and Devices", McGraw-Hill Higher Education, 2003.

[16] I. G. Mikellides, I. Katz, D. M. Goebel, And J. E. Polk, "Hollow Cathode Theory and Experiment. II. A Two-Dimensinal Theoretical Model of the Emitter Region," Journal Of Applied Physics 98, 2005.

[17] R. Liang, "The Combination of Two Concentric Discharge Channels Into a Nested Hall-Effect Thruster," M.S. Thesis, The University of Michigan, Cambridge, MI, USA, 2013.

[18] Ozturk, A.E.; Turkoz, E.; Ozgen, A.; Celik, M., "Design and Thermal Analysis of the Insert Region Heater of a Lanthanum Hexaboride Hollow Cathode," 6th International Conference On Recent Advances In Space Technologies (RAST), Istanbul, Turkey, June 2013

[19] O. Korkmaz, S. Jahanbakhsh, M. Celik, And H. Kurt, "Space Propulsion Research Vacuum Facility of the Bogazici University Space Technologies Laboratory," in 7th International Conference On Recent Advances in Space Technologies (RAST), Istanbul, Turkey, June 2015.

[20] Turan, N., Kokal, U., Kurt, H. and Celik, M., "Experimental Study of the Effects of the Cathode Position and the Electrical Circuit Configuration on the Operation of HK40 Hall Thruster and BUSTLab Hollow Cathode," 52nd Joint Propulsion Conference, Salt Lake City, UT, USA, July 2016, AIAA-2016-4834.

[21] Turan, N., Kokal, U. and Celik, M., "Experimental Investigation of the Effects of Cathode Current on HK40 Hall Thruster Operation," 5th Space Propulsion Conference, Rome, Italy, May 2016, also SP2016_ 3125333.